

Spatially Mapping the Spectral Density of a Single C₆₀ Molecule

Xinghua Lu, M. Grobis, K. H. Khoo, Steven G. Louie, and M. F. Crommie

*Department of Physics, University of California at Berkeley, Berkeley, California 94720-7300
and Materials Sciences Division, Lawrence Berkeley Laboratory, Berkeley, California 94720-7300*

(Received 22 July 2002; published 6 March 2003)

We have used scanning tunneling spectroscopy to spatially map the energy-resolved local density of states of individual C₆₀ molecules on the Ag(100) surface. Spectral maps were obtained for molecular states derived from the C₆₀ HOMO, LUMO, and LUMO + 1 orbitals, revealing new details of the spatially inhomogeneous C₆₀ local electronic structure. Spatial inhomogeneities are explained using *ab initio* pseudopotential density functional calculations. These calculations emphasize the need for explicitly including the C₆₀-Ag interaction and STM tip trajectory to understand the observed C₆₀ local electronic structure.

DOI: 10.1103/PhysRevLett.90.096802

PACS numbers: 73.22.-f, 71.15.-m, 73.63.-b

The most basic fullerene structure is the C₆₀ molecule. Since its discovery in 1985 [1], C₆₀ has been used as the fundamental component of a variety of new carbon nanostructures. Examples include endohedral fullerenes [2], peapod nanotubes [3], C₆₀ dimers [4], and single-molecule transistors [5]. Because of the potential for new applications, great efforts are being made to understand the physical and chemical properties of C₆₀ molecules on various substrates [6–12]. Much of this effort is aimed at determining how the C₆₀-substrate interaction alters local molecular electronic structure, and is an important step on the road toward creating controllable single-molecule technologies.

The electronic behavior of C₆₀ on various surfaces has been studied extensively using different techniques. Photoelectron spectroscopies have shown energy-level splitting in the highest occupied molecular orbital (HOMO) states and lowest unoccupied molecular orbital (LUMO) states for various monolayer systems [7]. X-ray diffraction has also been used to measure the orientation of C₆₀ molecules in monolayer systems [8]. Determining the *local* properties of isolated C₆₀ molecules, however, requires scanned probe microscopy. A number of STM studies have been performed to characterize the topographic structure of C₆₀ on different surfaces [9,10]. STM spectroscopic studies of C₆₀ have shown features associated with HOMO and LUMO states [11,12]. These spectroscopic measurements, however, were either spatially averaged or obtained at only one point on a molecule, and so ignore intramolecular spatial inhomogeneity in the electronic structure. Full characterization of the spatially inhomogeneous C₆₀ molecular states requires energy-resolved spectroscopic mapping, which has heretofore been lacking.

Here we report the first energy-resolved spectroscopic mapping of the molecular states of a single C₆₀ molecule at a metal surface. Using scanning tunneling spectroscopy we have spatially mapped the energy-resolved spectral density for the HOMO, LUMO, and LUMO + 1 states of C₆₀ on Ag(100). We observe strong spatial in-

homogeneity in the spectral density which reflects the structure and symmetry of C₆₀ molecular orbitals at different energies. In addition, we see enhanced splitting of the C₆₀ LUMO states in the vicinity of the Fermi energy (E_F) and are able to map out the spatial structure of molecular states near E_F . In order to understand the microscopic origin of this behavior, we have performed density functional theory (DFT) calculations for C₆₀ at a silver surface. Comparison between these calculations and experimental results gives us new insight into how C₆₀ electronic structure is modified via interaction with the Ag(100) surface and how this affects local density distributions. We find that precise comparison between experimental and theoretical images must take into account influences of the STM tip trajectory.

Our experiments were conducted using a homebuilt ultrahigh vacuum (UHV) STM. The single-crystal Ag(100) substrate was cleaned in UHV and dosed with C₆₀ after being cooled to 7 K. dI/dV spectra were measured through lock-in detection of the ac tunneling current driven by a 450 Hz, 10 mV (rms) signal added to the junction bias under open-loop conditions (bias voltage here is defined as the sample potential referenced to the tip). dI/dV images were acquired by positioning the STM tip at each point at constant current and then measuring dI/dV .

Figure 1 shows a representative 400 Å × 400 Å topograph of C₆₀ molecules on the Ag(100) surface ($V = 2.0$ V, $I = 0.3$ nA). Most C₆₀ molecules reside at Ag step edges with an apparent height of 5.7 ± 0.3 Å. We carefully examined ~90 C₆₀ molecules using many different tips and observed four distinct orientations, as shown in the insets. These topographs clearly resolve segmented structures on the C₆₀ molecule. Assuming the segments correspond to the pentagon rings of a C₆₀ molecular cage, we can deduce the orientation of the four molecules shown in the insets. From left to right, the topmost features are a 6:6 bond (i.e., the bond separating two adjacent hexagonal carbon rings), an apex atom, a hexagon ring, and a 5:6 bond (i.e., the bond separating a

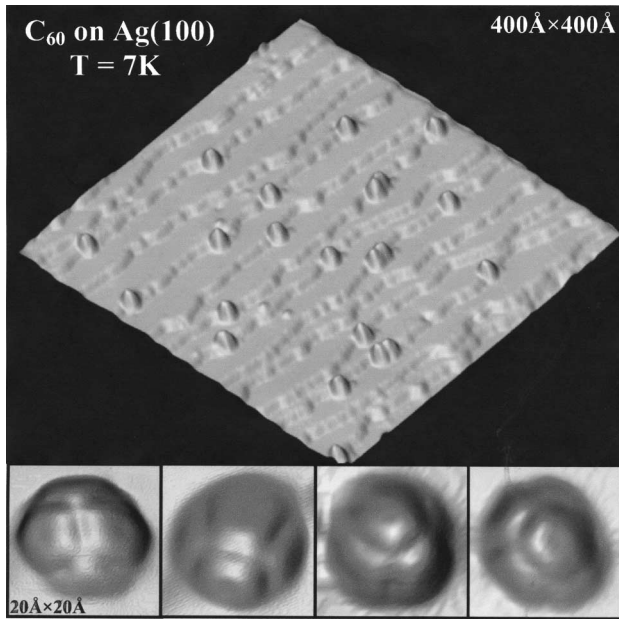


FIG. 1. Constant current topograph of C_{60} on Ag(100) at $T = 7$ K ($V = 2.0$ V, $I = 0.3$ nA). Insets: close-ups of the four observed molecular orientations.

pentagon ring and a hexagon ring). These orientations were observed with a distribution of 47%, 27%, 16%, and 10%, respectively.

In order to understand the local electronic structure of C_{60} adsorbates, we measured differential conductance (dI/dV) spectra at different sites on individual C_{60} molecules. Figure 2 shows typical dI/dV spectra measured at nine different spots over a single C_{60} molecule located at a Ag(100) step edge. These results were not sensitive to molecular orientation. The most striking features in the C_{60} spectra are three peaks centered at 1.62 ± 0.10 , 0.41 ± 0.03 , 0.02 ± 0.04 V, and a shoulder at -1.70 ± 0.30 V [13]. These resonances display strong spatial inhomogeneity, as shown by the variation in the spectra from point to point. Changes in the peak intensity of the resonance at 0.4 V appear to be inversely related to changes in the intensity of the peaks at 1.6 V and E_F .

The spatial inhomogeneity of the observed spectra for C_{60} arises from the local density of states (LDOS) distribution of the different molecular orbitals. Constant current STM topographs hint at this structure, but do not yield direct orbital resolution since they integrate over a number of molecular states. In order to experimentally untangle the behavior of individual C_{60} molecular orbitals, one must perform energy-resolved spectral mapping of the molecule. This is accomplished by spatially mapping dI/dV at a constant voltage over the molecule's surface. In the left side of Fig. 3 we present energy-resolved spectroscopic maps of one C_{60} molecule taken at the energies of the four resonances observed in our spectra (all images were acquired with the same tip). The dI/dV map of the highest energy resonance [1.6 V,

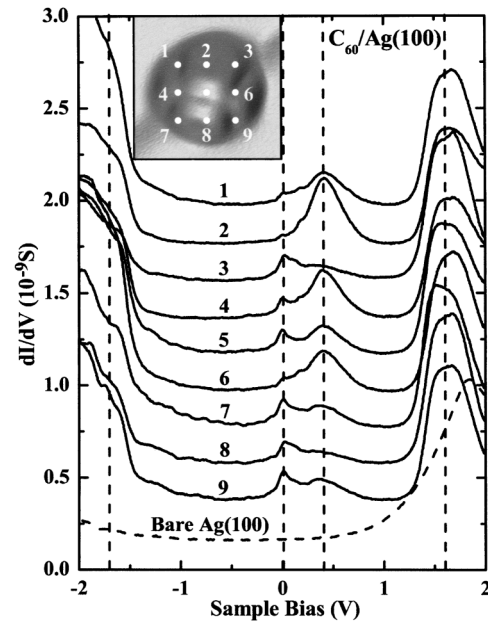


FIG. 2. dI/dV spectra of a single C_{60} on Ag(100) at $T = 7$ K. Spectra 1–9 were taken at indicated spots on the inset image and are shifted vertically for clarity. Tunneling parameters were $V = 2.0$ V, $I = 1.0$ nA before taking the spectra. The lowest spectrum was obtained from the bare Ag(100) surface and is not shifted.

Fig. 3(c)] shows clearly resolved “bright rings,” indicating LDOS buildup at the expected sites of C_{60} pentagon rings. At the 0.4 V resonance [Fig. 3(d)], however, we see a near inversion of the LDOS observed at 1.6 V. The spectral map of the E_F resonance shows nodal structure around the bright ring feature, while the map of the lowest energy state (-1.7 V shows a network of LDOS peaks displaced from the high density regions observed at other energies. Comparison of the dI/dV maps to constant current topographs [Figs. 3(b) and 3(g),] shows that the dI/dV maps reveal detail in the electronic structure that cannot be observed in topographs alone.

We have carried out *ab initio* pseudopotential density functional [14,15] calculations aimed at understanding the nature of the spatially varying electronic structure observed in our spectral mapping of C_{60} . These calculations were performed using the SIESTA code [16,17] with a double- ζ basis set and the local density approximation (LDA). Figure 4(a) shows the calculated spectrum of states for a free C_{60} molecule, which is consistent with previous DFT work [18]. The LDA HOMO-LUMO gap and LUMO-LUMO + 1 gap for free C_{60} are comparable to the energy separation between experimentally observed resonances. We note that owing to charge transfer from the Ag surface, the experimentally observed lowest LUMO states are partially occupied and lead to a smaller apparent HOMO-LUMO gap than that seen for a neutral C_{60} molecule. The free C_{60} theoretical spectrum, however, does not account for the strong splitting

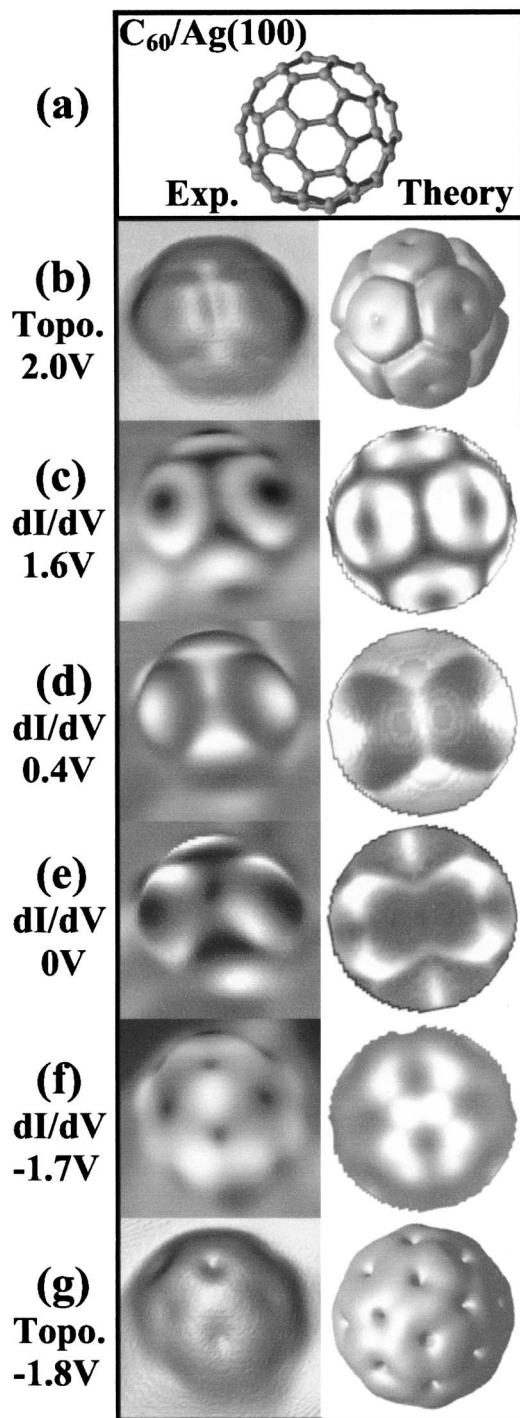


FIG. 3. Comparison of experimental scanning tunneling spectroscopy images of a single C_{60} molecule on Ag(100) with theory. Left column shows experimental results: (b) topograph taken at 2.0 V, (c)–(f) dI/dV maps taken at $V = 1.6$ V, 0.4 V, 0.0 V, -1.7 V, (g) topograph taken at -1.8 V. Right column shows results of DFT calculation: (b) simulated topograph for $V = 2.0$ V, (c)–(f) energy resolved electron density maps at $E = 1.2$ eV, 0.3 eV, 0.0 eV, -1.6 eV, (g) simulated topograph for $V = -1.8$ V. Constant current topographs are visualized as 3D rendered surfaces while experimental and calculated spectral maps are visualized as 2D projections.

experimentally observed among the LUMO states, where a difference of nearly 0.4 eV is observed between peaks, since it neglects the C_{60} -substrate interaction.

Modeling this interaction by simply deforming free C_{60} (up to 5%) or by applying an electric field to it (up to 0.5 V/Å) did not reproduce the observed splitting. Explicitly including the Ag substrate, however, produces a spreading of 0.4 eV in the LUMO states, closely reproducing what is seen experimentally. Figure 4(b) shows the calculated LDOS of a C_{60} molecule positioned with a 6:6 bond directly above a Ag(100) substrate atom. The electronic LDOS (averaged over a hemispherical shell of radius 5.5 Å) of the C_{60} molecule was calculated using eight k -points in the Brillouin zone of a supercell containing 200 surface atoms and four atomic layers of Ag. The C_{60} molecule and top layer of the substrate were allowed to relax, leading to a uniaxial elongation of the molecule by $\sim 1.6\%$ normal to the surface. We identify the experimentally observed resonances at E_F and 0.4 eV with local maxima of the LUMO states seen at 0.0 and 0.3 eV in this calculation. The calculated LUMO + 1 maximum is located at 1.2 eV above E_F , as compared to the experimentally observed state at 1.6 V. Agreement between experimental and theoretical spectra in Fig. 4 is quite good, and the remaining differences are consistent

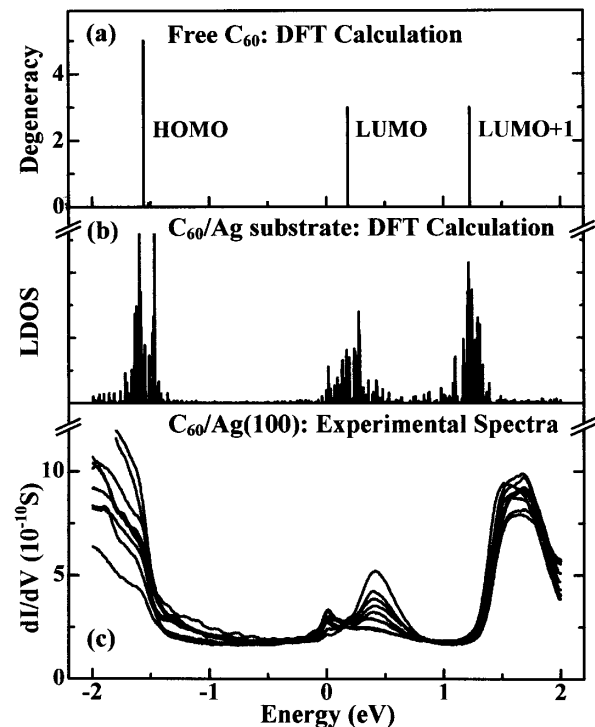


FIG. 4. Calculated density of states for (a) a free C_{60} molecule, and (b) an individual C_{60} molecule adsorbed to a Ag(100) substrate (LDOS here is integrated over a 5.5 Å radius hemispherical shell above the C_{60} molecule for states associated with 8 different k points). (c) Experimental C_{60} dI/dV spectra from Fig. 2 (curves not vertically shifted here).

with expected quasiparticle self-energy corrections, which enlarge the gap between occupied and unoccupied levels as well as quasiparticle level spacings as compared to LDA eigenvalues [19].

In order to check the orbital assignments, we compared the spatial distribution of calculated molecular states (ranging from HOMO to LUMO + 1) with the experimentally determined spectral maps. Energy-resolved images of the calculated $C_{60}/Ag(100)$ states at 1.2, 0.3, 0.0, and -1.6 eV (with respect to E_F) can be seen on the right side of Fig. 3. In order to account for the actual trajectory of the STM tip [20], the theoretical images were obtained by calculating the energy-resolved electronic LDOS on a simulated constant current surface. Such constant current surfaces were generated by integrating the LDOS from E_F to the bias voltage, and reproduce experimental topographs nicely [Figs. 3(b) and 3(g)]. The energy-resolved LDOS maps account well for the experimentally observed spatial and energetic variations in spectral density. The bright ring structures observed in experimental dI/dV maps of the LUMO + 1 state are confirmed to originate from pentagon rings, while bright antinodes in the dI/dV map of the HOMO state are seen to originate from 6:6 double bonds. The experimentally observed nodal structure of the low energy LUMO state is reproduced in the calculation, as well as a density inversion between LUMO and LUMO + 1 states.

We also performed the simpler theoretical procedure of calculating LDOS density maps over a hemisphere of constant radius around the C_{60} molecule. This reproduced the main features of the dI/dV maps at -1.7 , 0.0 , 1.6 V, but was completely unable to account for the density inversion seen at 0.4 V. The dI/dV map at this energy can be reconciled only with actual molecular electronic structure by taking into account the fact that experimentally the STM tip actually travels over a contour of constant energy-integrated LDOS, rather than a perfect hemisphere. Though an LDOS inversion exists on this contour, there is no global LDOS inversion between the 0.4 and 1.6 V states.

In conclusion, we have measured the orientation and electronic structure of individual C_{60} molecules at the Ag(100) surface. We observe strong spatial inhomogeneity over the surface of a single molecule, and strong splitting of spectroscopic peaks. Spatial variations in C_{60} spectral density were mapped using energy-resolved STM imaging techniques for the first time. These results can be understood using LDA calculations that emphasize the important role played by the Ag substrate in modifying the electronic structure of adsorbed C_{60} . Some molecular features seen in C_{60} spectroscopic maps, however, can be understood only by accounting for the trajectory of the STM tip. This has general implications for the interpretation of STM spectral maps of electronically inhomogeneous molecular systems.

This work was supported in part by NSF Grant No. DMR00-87088 and by the Director, Office of Energy Research, Office of Basic Energy Science, Division of Material Sciences and Engineering, U.S. Department of Energy under Contracts No. DE-AC03-76SF0098 and No. DE-AC03-76F00098. Computational resources have been provided by DOE at the National Energy Research Scientific Computing Center.

-
- [1] H.W. Kroto *et al.*, Nature (London) **318**, 162 (1985).
 - [2] T. Ohtsuki *et al.*, Phys. Rev. Lett. **77**, 3522 (1996); T. Ohtsuki *et al.*, Phys. Rev. Lett. **81**, 967 (1998).
 - [3] B.W. Smith *et al.*, Nature (London) **396**, 323 (1998); D. J. Hornbaker *et al.*, Science **295**, 828 (2002).
 - [4] G. Wang *et al.*, Nature (London) **387**, 583 (1997).
 - [5] H. Park *et al.*, Nature (London) **407**, 57 (2000).
 - [6] S. J. Chase *et al.*, Phys. Rev. B **46**, 7873 (1992); S. Suto *et al.*, Phys. Rev. B **56**, 7439 (1997); H. Wang *et al.*, Surf. Sci. **442**, L1024 (1999); S. Rogge *et al.*, Carbon **38**, 1647 (2000); C. Cepek *et al.*, Phys. Rev. Lett. **86**, 3100 (2001).
 - [7] A. J. Maxwell *et al.*, Phys. Rev. B **57**, 7312 (1998); K. Sakamoto *et al.*, Phys. Rev. B **58**, 13951 (1998); A. J. Maxwell *et al.*, Phys. Rev. Lett. **79**, 1567 (1997); D. Purdie *et al.*, Surf. Sci. **364**, 279 (1996).
 - [8] M. Pedio *et al.*, Phys. Rev. Lett. **85**, 1040 (2000); R. Fasel *et al.*, Phys. Rev. Lett. **76**, 4733 (1996).
 - [9] R. Z. Bakhtizin *et al.*, Phys. Usp. **40**, 275 (1997), and references therein; P.W. Murray *et al.*, Phys. Rev. B **55**, 9360 (1997); J. Weckesser *et al.*, Phys. Rev. B **64**, 161403 (2001).
 - [10] J. G. Hou *et al.*, Phys. Rev. Lett. **83**, 3001 (1999); J. I. Pascual *et al.*, Chem. Phys. Lett. **321**, 78 (2000); H. Wang *et al.*, Phys. Rev. B **63**, 085417 (2001).
 - [11] D. Porath *et al.*, Phys. Rev. B **56**, 9829 (1997).
 - [12] A. W. Dunn *et al.*, Surf. Sci. **498**, 237 (2002); X. Yao *et al.*, Surf. Sci. **366**, L743 (1996); M. K.-J. Johansson *et al.*, Phys. Rev. B **54**, 13472 (1996); T. David *et al.*, Phys. Rev. B **50**, 5810 (1994).
 - [13] Similar behavior was observed for terrace molecules, but our statistics for them are poor since they account for less than 5% of all observed molecules. In addition, terrace molecules often bind to defects that change their electronic response.
 - [14] W. Kohn and L. J. Sham, Phys. Rev. **136**, A1133 (1965).
 - [15] S. G. Louie, *Electronic Structure, Dynamics, and Quantum Structure Properties of Condensed Matter*, edited by J. T. Devreese and P. Van Camp (Plenum, New York, 1985).
 - [16] D. S. Portal *et al.*, Int. J. Quantum Chem. **65**, 453 (1997).
 - [17] N. Troullier and J. L. Martins, Phys. Rev. B **43**, 1993 (1991).
 - [18] S. Saito and A. Oshiyama, Phys. Rev. Lett. **66**, 2637 (1991); E. L. Shirley and S. G. Louie, Phys. Rev. Lett. **71**, 133 (1993).
 - [19] M. S. Hybersten and S. G. Louie, Phys. Rev. B **34**, 5390 (1986).
 - [20] G. Hörmandinger, Phys. Rev. Lett. **73**, 910 (1994).